

Regular article

## Large Field and Small Field Inflation Models in Confrontation with Planck2018 and BICEP2018 Datasets

Mozhdeh Bitaj<sup>1</sup> · Narges Rashidi<sup>2</sup> · Kourosh Nozari<sup>3</sup>

<sup>1</sup> Department of Theoretical Physics, Faculty of Science, University of Mazandaran, P. O. Box 47416-95447, Babolsar, Iran;  
E-mail: mozhdeh.bitaj@gmail.com

<sup>2</sup> Department of Theoretical Physics, Faculty of Science, University of Mazandaran, P. O. Box 47416-95447, Babolsar, Iran;  
E-mail: n.rashidi@umz.ac.ir

<sup>3</sup> Department of Theoretical Physics, Faculty of Science, University of Mazandaran, P. O. Box 47416-95447, Babolsar, Iran;  
Corresponding author E-mail: knozari@umz.ac.ir

Received: October 02, 2023; Revised: October 30, 2023; Accepted: November 02, 2023.

**Abstract.** We study the non-minimal inflation with both the large field and small field potentials in the context of the new observational data. We analyze the linear and non-linear perturbations to obtain the scalar spectral index, tensor-to-scalar ratio, and nonlinearity parameter. By performing a numerical analysis on the scalar spectral index and tensor-to-scalar ratio, and comparing the results with Planck2018 TT, TE, EE+lowE+lensing+BAO+BK14(18) data, we find that the non-minimal large field inflation is observationally viable if the non-minimal coupling parameter is of the order of  $10^{-3}$ . The same analysis on the non-minimal small field inflation gives the values for the non-minimal coupling parameter as  $10^{-4}$ . We also study the non-Gaussian features in both equilateral and orthogonal configurations for large and small field potentials and find small values for these amplitudes, consistent with Planck2018 TTT, EEE, TTE and EET data. We show that the absolute values of the non-linearity parameter,  $f_{NL}$ , is larger in large field inflation than the small field model for both configurations. Also, we obtain more severe constraints on the parameter  $p$  in the introduced large field and small field potentials with respect to previously reported constraints.

*Keywords:* Non-Minimal Inflation; Large Field Inflation; Small Field Inflation; Non-Gaussianity; Observational Constraints.

---

**COPYRIGHTS:** ©2023, Journal of Holography Applications in Physics. Published by Damghan University. This article is an open-access article distributed under the terms and conditions of the Creative Commons Attribution 4.0 International (CC BY 4.0).  
<https://creativecommons.org/licenses/by/4.0>



# 1 Introduction

Inflation was first presented as a paradigm to solve some of the inadequacies of the standard model of cosmology [1, 2, 3, 4, 5, 6, 7, 8]. In the simple single-field inflation model, the dominant of the field's potential on the kinetic term leads to an exponential expansion of the universe with almost scale-invariant and Gaussian amplitude of the primordial perturbations [9]. However, there are also some other extended models of inflation which lead to interesting cosmological results. One successful and essentially inevitable class of the extended inflationary models is a model where the scalar field and the curvature scalar  $R$  are non-minimally coupled. This coupling seems necessary for the renormalization term arising in quantum field theory in curved space [10]. This term arises at the quantum level when we consider the quantum corrections to the scalar field theory [11, 12]. To have gravity as a spontaneous symmetry-breaking effect, the presence of non-minimal coupling is important [13, 14]. Also, the oscillating Universe is possible with a NMC term in the action [15]. Therefore, it seems that considering the nonminimal coupling between the scalar field and Ricci scalar leads to interesting results. To see some works about the non-minimal coupling models see [16, 17, 18, 19, 20, 21, 22, 23].

Although several works have been done on the non-minimal inflation issue, the new data might change the viability of the models or their observational constraints. For instance, the Planck2018 TT, TE, EE+lowE+lensing+BAO+BK14 data gives the value  $n_s = 0.9658 \pm 0.0038$  for the scalar spectral index, based on the  $\Lambda$ CDM +  $r + \frac{dn_s}{d \ln k}$  model [24, 25]. This data gives the upper bound on the tensor-to-scalar ratio as  $r < 0.072$  [24, 25]. However, Planck2018 TT, TE, EE+lowE+lensing+BAO+BK18 data implies more tighter bound on the tensor-to-scalar ratio as  $r < 0.036$  [26, 27]. By these constraints, it seems interesting to revisit the non-minimal inflation and obtain some new viable domains of the model's parameters. In studying non-minimal inflation, we consider the non-minimal function as  $f = \xi \phi^2$ , where  $\xi$  is a constant parameter. We also consider two types of potential corresponding to the Large Field Inflation (LFI) and Small Field Inflation (SFI). We shall see that although the minimal LFI with  $N = 60$  is not consistent with observational data, the non-minimal coupling makes it viable.

Another important aspect of the inflation model is the non-Gaussian feature of its primordial perturbations. By considering the three-point correlation function and finding the amplitude of the non-Gaussianity, it is possible to check the viability of the model from this perspective. There are some constraints on the amplitudes of the non-Gaussianity from the observational data. Planck2018 TTT, EEE, TTE and EET data gives the values of the equilateral and orthogonal amplitudes of the non-Gaussianity as  $f_{NL}^{equil} = -26 \pm 47$  and  $f_{NL}^{ortho} = -38 \pm 24$ , respectively [28]. In this paper, we seek the non-Gaussianity feature in the LFI and SFI models with non-minimal coupling. We show that the predictions for the equilateral and orthogonal amplitudes of the non-Gaussianity in these models are small values.

The paper is organized as follows: Section 2 is the setup of the model where we present the background equations and the slow-roll parameters in our model. In section 3 we briefly study the linear and non-linear perturbations in this model. In section 4, by considering the LFI and SFI models, we perform a numerical analysis on the model and obtain some constraints on the parameters along with some comparison between LFI and SFI results. Section 5 is devoted to a summary and conclusion.

## 2 The Setup

The action for a model where a scalar field is non-minimally coupled to the Ricci scalar is given by

$$S = \int d^4x \sqrt{-g} \left[ \frac{1}{2\kappa^2} R + f(\phi)R - \frac{1}{2} \partial_\mu \phi \partial^\mu \phi - V(\phi) \right], \quad (1)$$

where  $R$  is the Ricci scalar,  $\phi$  is a scalar field (inflaton) with the potential  $V(\phi)$ , and  $f(\phi)$  is a general function of the scalar field. By considering the FRW metric, the Friedmann equation corresponding to the action (1) is

$$H^2 (1 + 2\kappa^2 f) = \frac{\kappa^2}{3} \left( \frac{1}{2} \dot{\phi}^2 - 6Hf'\dot{\phi} + V(\phi) \right), \quad (2)$$

where, a dot refers to a time derivative of the parameter and a prime denotes a derivative with respect to the scalar field. The equation of motion of the scalar field, obtained from the variation of action (1) with respect to the scalar field is given by

$$\ddot{\phi} + 3H\dot{\phi} - 6f'R + V' = 0. \quad (3)$$

In this model, the slow-roll parameters, which are defined as  $\epsilon \equiv -\frac{\dot{H}}{H^2}$  and  $\eta = -\frac{1}{H} \frac{\ddot{H}}{\dot{H}}$ , take the following forms

$$\epsilon = \frac{A}{1 + 2\kappa^2 f}, \quad (4)$$

$$\eta = \frac{2A}{1 + 2\kappa^2 f} - \frac{\dot{A}}{H\epsilon(1 + 2\kappa^2 f)} + \frac{A}{H\epsilon} \frac{2\kappa^2 f'\dot{\phi}}{(1 + 2\kappa^2 f)^2}, \quad (5)$$

where,

$$A \equiv \frac{\kappa^2 \dot{\phi}^2}{2H^2} - \frac{\kappa^2 f'\dot{\phi}}{H} + \frac{\kappa^2 f''\dot{\phi}^2}{H^2} + \frac{\kappa^2 f'\ddot{\phi}}{H^2}. \quad (6)$$

The inflationary expansion implies  $\epsilon \ll 1$  and  $|\eta| \ll 1$ , and as soon as one of these parameters meets unity, the inflationary phase terminates. The number of e-folds is another important parameter which is defined as

$$N = \int_{t_{hc}}^{t_f} H dt, \quad (7)$$

and in the non-minimal model is given by

$$N \simeq \int_{\phi_{hc}}^{\phi_f} \frac{3H^2}{V' - 6f'R} d\phi, \quad (8)$$

where the subscripts  $hc$  and  $f$  denote the time of the horizon crossing of the physical scale and the end of the inflation respectively. To have a successful inflation scenario, it seems at least 60 e-folds are needed. After presenting the background equations in this section, we study the perturbations in the following.

### 3 Primordial Perturbation

In this section, we study cosmological perturbations in the non-minimal model. By considering the scalar part of the perturbed metric in the ADM formalism as [29, 30, 31]

$$ds^2 = -(1 + 2\Phi)dt^2 + 2a(t)B_{,i} dt dx^i + a^2(t)(1 - 2\Psi)\delta_{ij}dx^i dx^j, \quad (9)$$

where  $\Phi$  and  $B$  are 3-scalar, and  $\Psi$  is the spatial curvature perturbation, we expand the action (1) up to the second order in perturbation as

$$S_2 = \int dt d^3x a^3 \mathcal{W} \left[ \dot{\Psi}^2 - \frac{c_s^2}{a^2} (\partial\Psi)^2 \right], \quad (10)$$

where the parameter  $\mathcal{W}$  is defined as

$$\mathcal{W} = \frac{(\kappa^{-2} + f)^2 \left( \frac{9}{\kappa^2} H^2 (1 + \kappa^2 f) - \frac{3\dot{\phi}^2}{2} + 18H\dot{\phi}f' \right)}{-\frac{1}{4} \left( 2\kappa^{-2} H (1 + \kappa^2 f) + 2\dot{\phi}f' \right)^2} + 3(\kappa^{-2} + f), \quad (11)$$

and the square of the sound speed is given by

$$c_s^2 = 3 \left[ 2 \left( 2\kappa^{-2} H (1 + \kappa^2 f) + 2\dot{\phi}f' \right) (\kappa^{-2} + f)^2 H - \left( 2\kappa^{-2} H (1 + \kappa^2 f) + 2\dot{\phi}f' \right)^2 (\kappa^{-2} + f) \right. \\ \left. + 4 \left( 2\kappa^{-2} H (1 + \kappa^2 f) + 2\dot{\phi}f' \right) (\kappa^{-2} + f) \dot{\phi}f' - 2 \left( \kappa^{-2} + f \right)^2 \frac{d(2\kappa^{-2} H (1 + \kappa^2 f) + 2\dot{\phi}f')}{dt} \right] \\ \left[ \left( 9 \left( 2\kappa^{-2} H (1 + \kappa^2 f) + 2\dot{\phi}f' \right)^2 - 4 \left( \kappa^{-2} + f \right) \left( 9\kappa^{-2} H^2 (1 + \kappa^2 f) - \frac{3}{2} \dot{\phi}^2 + 18H\dot{\phi}f' \right) \right) \right]^{-1}. \quad (12)$$

In surveying the perturbations of a model, by studying the scalar spectral index we find some useful information about the primordial perturbations. To obtain this parameter, by calculating the vacuum expectation value of  $\Psi$  at  $\tau = 0$  as [32, 33, 34, 35]

$$\langle 0 | \Psi(0, \mathbf{k}_1) \Psi(0, \mathbf{k}_2) | 0 \rangle = (2\pi)^3 \delta^3(\mathbf{k}_1 + \mathbf{k}_2) \frac{2\pi^2}{k^3} \mathcal{A}_s, \quad (13)$$

where the power spectrum  $\mathcal{A}_s$  is given by

$$\mathcal{A}_s = \frac{H^2}{8\pi^2 \mathcal{W} c_s^3}. \quad (14)$$

The scalar spectral index of the perturbations at the Hubble crossing is defined as

$$n_s - 1 = \left. \frac{d \ln \mathcal{A}_s}{d \ln k} \right|_{c_s k = aH}, \quad (15)$$

which in the non-minimal model takes the following form

$$n_s - 1 = -2\epsilon - \frac{5\kappa^2 f' \dot{\phi}}{2H(1 + \kappa^2 f)} - \frac{1}{H} \frac{d \ln \left( \epsilon + \frac{5\kappa^2 f' \dot{\phi}}{4H(1 + \kappa^2 f)} \right)}{dt} - \frac{1}{H} \frac{d \ln c_s}{dt}. \quad (16)$$

If we repeat the procedure by considering the tensor part of the perturbations, we find the amplitude of the tensor perturbations as follows

$$\mathcal{A}_T = \frac{H^2}{2\pi^2 \mathcal{W}_T}, \quad (17)$$

where

$$\mathcal{W}_T = \frac{1}{4\kappa^2}. \quad (18)$$

By using the definition of the tensor spectral index as

$$n_T = \frac{d \ln \mathcal{A}_T}{d \ln k}, \quad (19)$$

we obtain

$$n_T = -2\epsilon - \frac{\kappa^2 f' \dot{\phi}}{2H(1 + \kappa^2 f)}. \quad (20)$$

Finally, we can get the ratio between the amplitudes of the tensor and scalar perturbations (tensor-to-scalar ratio) as

$$r = \frac{\mathcal{A}_T}{\mathcal{A}_s} = 16c_s \left( \epsilon + \frac{5\kappa^2 f' \dot{\phi}}{4H(1 + \kappa^2 f)} \right). \quad (21)$$

We can also continue our study to the higher order in perturbations to survey the non-Gaussian feature in our model. By expanding the action (10) up to the third order we find

$$\begin{aligned} S_3 = \int dt d^3x \left\{ \left[ -\frac{3a^3}{\kappa^2} \left( \frac{1 + \kappa^2 f}{c_s^2} \right) \left( \frac{1}{c_s^2} - 1 \right) \left( \epsilon + \frac{5\kappa^2 f' \dot{\phi}}{4H(1 + \kappa^2 f)} \right) \right] \Psi \dot{\Psi} + \left[ \frac{a}{\kappa^2} \left( 1 + \kappa^2 f \right) \right. \right. \\ \left. \left. \left( \frac{1}{c_s^2} - 1 \right) \left( \epsilon + \frac{5\kappa^2 f' \dot{\phi}}{4H(1 + \kappa^2 f)} \right) \right] \Psi (\partial \Psi)^2 + \left[ \frac{a^3}{\kappa^2} \left( \frac{1 + \kappa^2 f}{c_s^2 H} \right) \left( \frac{1}{c_s^2} - 1 \right) \left( \epsilon + \frac{5\kappa^2 f' \dot{\phi}}{4H(1 + \kappa^2 f)} \right) \right] \right. \\ \left. \dot{\Psi}^3 - \left[ a^3 \frac{2}{c_s^2} \left( \epsilon + \frac{5\kappa^2 f' \dot{\phi}}{4H(1 + \kappa^2 f)} \right) \dot{\Psi} (\partial_i \Psi) (\partial_i \mathcal{X}) \right] \right\}. \quad (22) \end{aligned}$$

Now, the three-point operator in the conformal time interval between the beginning and end of the inflation for  $\Psi$  is defined as [9, 34, 35]

$$\langle \Psi(\mathbf{k}_1) \Psi(\mathbf{k}_2) \Psi(\mathbf{k}_3) \rangle = -i \int_{\tau_i}^{\tau_f} d\tau a \langle 0 | [\Psi(\tau_f, \mathbf{k}_1) \Psi(\tau_f, \mathbf{k}_2) \Psi(\tau_f, \mathbf{k}_3), H_{int}(\tau)] | 0 \rangle, \quad (23)$$

where the interacting Hamiltonian,  $H_{int}$ , is equal to the Lagrangian of the third order action. Solving the integral gives us the following three-point correlation function

$$\langle \Psi(\mathbf{k}_1) \Psi(\mathbf{k}_2) \Psi(\mathbf{k}_3) \rangle = (2\pi)^3 \delta^3(\mathbf{k}_1 + \mathbf{k}_2 + \mathbf{k}_3) \mathcal{B}_\Psi(\mathbf{k}_1, \mathbf{k}_2, \mathbf{k}_3), \quad (24)$$

with

$$\mathcal{B}_\Psi(\mathbf{k}_1, \mathbf{k}_2, \mathbf{k}_3) = \frac{(2\pi)^4 \mathcal{A}_s}{\prod_{i=1}^3 k_i^3} \mathcal{E}_\Psi(\mathbf{k}_1, \mathbf{k}_2, \mathbf{k}_3). \quad (25)$$

$\mathcal{A}_s$  in equation (25) is given by equation (14). Also, the parameter  $\mathcal{E}_\Psi$  is defined as

$$\mathcal{E}_\Psi = \frac{3}{4} \left( 1 - \frac{1}{c_s^2} \right) \mathcal{S}_1 + \frac{1}{4} \left( 1 - \frac{1}{c_s^2} \right) \mathcal{S}_2 + \frac{3}{2} \left( \frac{1}{c_s^2} - 1 \right) \mathcal{S}_3, \quad (26)$$

where

$$\mathcal{S}_1 = \frac{2}{K} \sum_{i>j} k_i^2 k_j^2 - \frac{1}{K^2} \sum_{i \neq j} k_i^2 k_j^3, \quad (27)$$

$$\mathcal{S}_2 = \frac{1}{2} \sum_i k_i^3 + \frac{2}{K} \sum_{i>j} k_i^2 k_j^2 - \frac{1}{K^2} \sum_{i \neq j} k_i^2 k_j^3, \quad (28)$$

$$\mathcal{S}_3 = \frac{(k_1 k_2 k_3)^2}{K^3}, \quad (29)$$

and

$$K = k_1 + k_2 + k_3. \quad (30)$$

To measure the amplitude of the non-Gaussianity, we define the nonlinearity parameter  $f_{NL}$  as

$$f_{NL} = \frac{10}{3} \frac{\mathcal{E}_\Psi}{\sum_{i=1}^3 k_i^3}. \quad (31)$$

Now, we consider two shapes of the non-Gaussianity which are almost orthogonal. These two are the equilateral (corresponding to  $k_1 = k_2 = k_3$  limit) and the orthogonal shapes and are given by [36]

$$\check{\mathcal{S}}^{equi} = -\frac{12}{13} (3\mathcal{S}_1 - \mathcal{S}_2), \quad (32)$$

and

$$\check{\mathcal{S}}^{ortho} = \frac{12}{14 - 13\beta} (\beta(3\mathcal{S}_1 - \mathcal{S}_2) + 3\mathcal{S}_1 - \mathcal{S}_2), \quad (33)$$

where,  $\beta \simeq 1.1967996$ . If we write the bispectrum (26) in terms of the equilateral and orthogonal basis as

$$\mathcal{E}_\Psi = \mathcal{C}_1 \check{\mathcal{S}}^{equi} + \mathcal{C}_2 \check{\mathcal{S}}^{ortho}, \quad (34)$$

with following definitions for  $\mathcal{C}_1$  and  $\mathcal{C}_2$

$$\mathcal{C}_1 = \frac{13}{12} \left[ \frac{1}{24} \left( 1 - \frac{1}{c_s^2} \right) (2 + 3\beta) \right], \quad (35)$$

and

$$\mathcal{C}_2 = \frac{14 - 13\beta}{12} \left[ \frac{1}{8} \left( 1 - \frac{1}{c_s^2} \right) \right], \quad (36)$$

we find the equilateral and orthogonal amplitudes of the non-Gaussianity as

$$f_{NL}^{equi} = \frac{325}{18} \left[ \frac{1}{24} \left( \frac{1}{c_s^2} - 1 \right) (2 + 3\beta) \right], \quad (37)$$

and

$$f_{NL}^{ortho} = \frac{10}{9} \left( \frac{65}{4} \beta + \frac{7}{6} \right) \left[ \frac{1}{8} \left( 1 - \frac{1}{c_s^2} \right) \right]. \quad (38)$$

Having these amplitudes of the non-Gaussianity helps us to complete our study on the non-minimal inflation model. In this regard, in the next section, we perform some numerical analysis on the perturbations parameter  $n_s$  and  $r$  and also, non-Gaussian parameters  $f_{NL}^{equil}$  and  $f_{NL}^{ortho}$  to compare the results for LFI and SFI models with observational data.

## 4 Observational Constraints

In this section, we seek the observational viability of the model. To this end, we adopt some functions for the non-minimal coupling and potential. We choose a non-minimal function as  $f(\phi) = \xi \phi^2$ . For the potential, we consider two types of potential corresponding to the large field inflation and small field inflation. With these adoptions, we study the model numerically to examine the viability of this model.

### 4.1 Large Field Inflation

Large field inflation models are the simplest inflation models with single-term potentials [37, 38]. In these models, the scalar field, starting from a maximum value ( $\Delta\phi > M_{pl}$ ), rolls slowly towards the minimum of the potential at  $\phi = 0$ , where the field starts oscillating. If the transformation of the field is super Planckian, the generated gravitational waves can be large enough to be observed in the near future. The potential corresponding to a LFI model is defined as follows

$$V(\phi) = M^4 \left( \frac{\phi}{M_{pl}} \right)^p \quad (39)$$

where the parameter  $M$  is the mass scale which is fixed by CMB polarization. Also,  $p$  is the free parameter that can be constrained with observational data. However, to satisfy the condition  $\Delta\phi > M_{pl}$ , the value of  $p$  should be in the range  $[0.2, 5]$ , see for instance [37, 38]. By using this potential, we perform numerical analysis on the scalar spectral index and tensor-to-scalar ratio to find the ranges of the model's parameters that give the observationally viable values of  $r$  and  $n_s$ . The result is shown in figure 1. To plot this figure, we have used the constraints  $n_s = 0.9658 \pm 0.0038$  and  $r < 0.072$  from Planck2018 TT, TE, EE+lowE+lensing+BAO+BK14 [24, 25], and  $r < 0.036$  from Planck2018 TT, TE, EE+lowE+lensing+BAO+BK18 datasets [26, 27]. Note that, in the figure, the blue region overlaps with some domain of the green region. To show the observational viability more clearly, we have plotted  $r - n_s$  behavior in the background of both Planck2018 TT, TE, EE+lowE+lensing+BAO+BK14 and Planck2018 TT, TE, EE+lowE+lensing+BAO+BK18 datasets in figure 2. According to our analysis, the non-minimal LFI is consistent with Planck2018 TT, TE, EE+lowE+lensing+BAO+BK14 data if  $p \leq 0.92$  at 68% CL and if  $p \leq 1.05$  at 95% CL. The model is consistent with Planck2018 TT, TE, EE+lowE+lensing+BAO+BK18 data if  $p \leq 0.69$  at 68% CL and if  $p \leq 0.080$  at 95% CL. We have also obtained the constraints on the non-minimal coupling parameter  $\xi$  for some sample values of  $p$  which have been summarized in table 1. It is important to notice that the minimal LFI with  $N = 60$  is not consistent with observation. The non-minimal coupling makes LFI observationally viable. It is also possible to check the prediction of the LFI model in equilateral and orthogonal amplitudes of non-Gaussianity. The numerical predictions for these amplitudes are shown in figure 3. From Planck2018 TTT, EEE, TTE and EET data we have  $f_{NL}^{equil} = -27 \pm 47$  and  $f_{NL}^{ortho} = -38 \pm 24$  [28]. Therefore, the prediction of the LFI model for non-Gaussianity is consistent with the observational data.

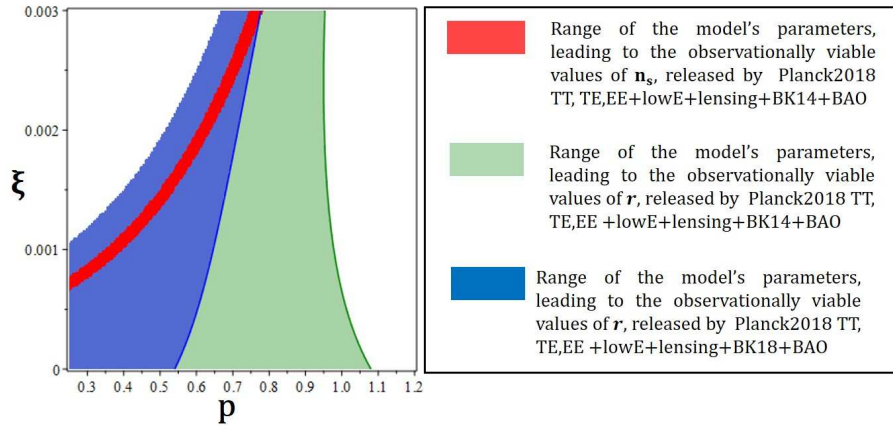


Figure 1: The ranges of the parameters  $\xi$  and  $p$  in the LFI model, leading to the observationally viable values of  $n_s$  and  $r$ .

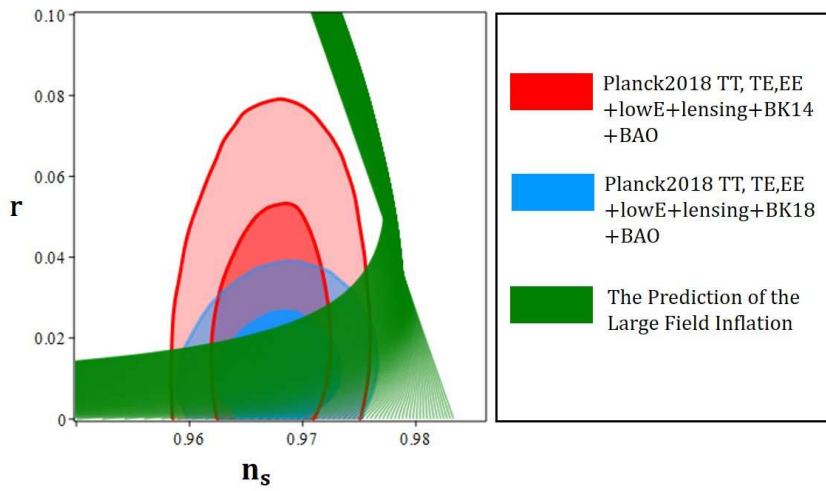


Figure 2:  $r - n_s$  behavior in the LFI model, in the background of the several dataset.



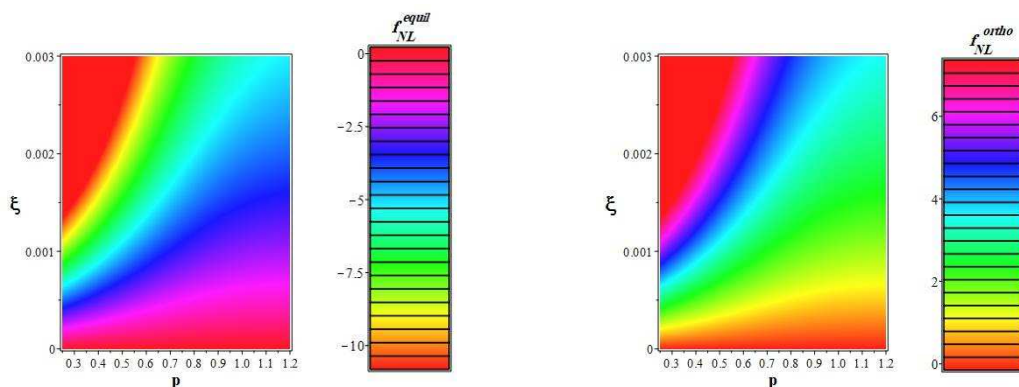


Figure 3: The prediction of the LFI model for equilateral and orthogonal amplitudes of the non-Gaussianity.

## 4.2 Small Field Inflation

In the Small Field Inflation models, the scalar field starts from the small values and rolls slowly to the large values. The SFI is Sub-Planckian ( $\Delta\phi < M_{pl}$ ) model [37, 38]. The potential of the SFI is given by

$$V(\phi) = M^4 \left[ 1 - \left( \frac{\phi}{\mu} \right)^p \right], \quad (40)$$

where the mass scale  $\mu$  is in the range  $\log\left(\frac{\mu}{M_{pl}}\right) \in [-1, 0]$  and  $p \in [2, 10]$ . With this potential also, we perform numerical analysis on the scalar spectral index and tensor-to-scalar ratio to find the ranges of the model's parameters that give the observationally viable values of  $r$  and  $n_s$ . Figure 4 shows the observationally viable ranges of the model's parameters. Note that, in this figure, the blue and green regions are overlapped. The behavior of  $r - n_s$  in the background of both Planck2018 TT, TE, EE+lowE+lensing+BAO+BK14 and Planck2018 TT, TE, EE+lowE+lensing+BAO+BK18 datasets is shown in figure 5. Although we consider the non-minimal coupling, the tensor-to-scalar ratio with small field potential is yet small. By performing the numerical analysis, we have found that the non-minimal SFI is consistent with Planck2018 TT, TE, EE+lowE+lensing+BAO+BK14 data if  $p \geq 9.1$  at 68% CL and  $p \geq 6.2$  at 95% CL. Also there is consistency with Planck2018 TT, TE, EE+lowE+lensing+BAO+BK18 data if  $p \geq 7$  at 68% CL and  $p \geq 6.2$  at 95% CL. The constraints on the parameter  $\xi$ , for some sample values of  $p$ , are presented in table 2. The prediction of the SFI model in equilateral and orthogonal amplitudes of non-Gaussianity is shown in figure 6. In this case also, the values of these amplitudes are small but consistent with observational data.

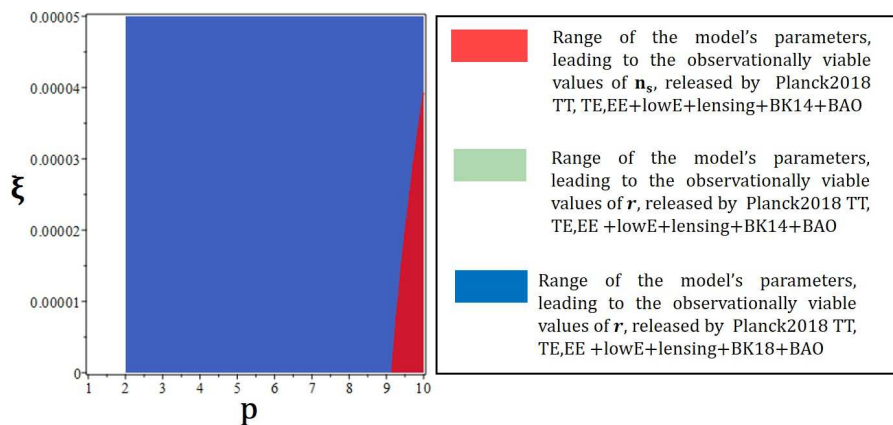


Figure 4: The ranges of the parameters  $\xi$  and  $p$  in the SFI model, leading to the observationally viable values of  $n_s$  and  $r$ .

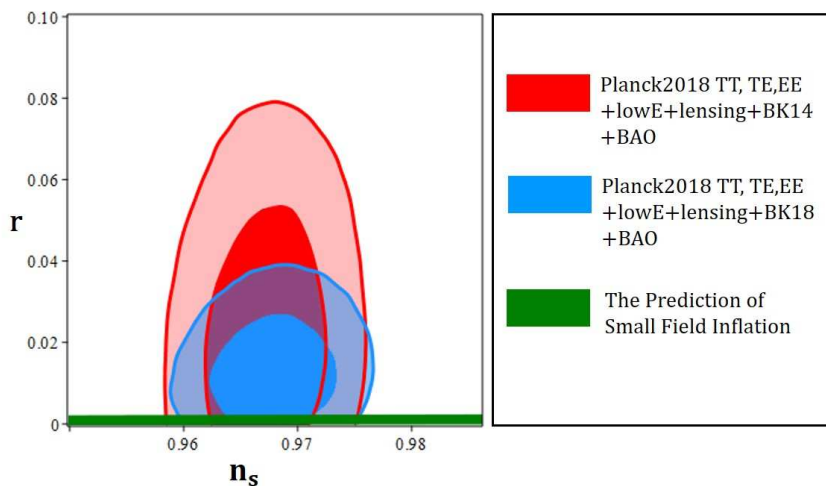


Figure 5:  $r - n_s$  behavior in the SFI model, in the background of the several dataset.

Table 1: The ranges of the parameter  $\xi$  in which the tensor-to-scalar ratio and the scalar spectral index of the non-minimal LFI are consistent with different data sets.

$p$	Planck2018 TT, TE, EE+lowE+lensing+BK14+BAO	Planck2018 TT, TE, EE+lowE+lensing+BK14+BAO	Planck2018 TT, TE, EE+lowE+lensing+BK18+BAO	Planck2018 TT, TE, EE+lowE+lensing+BK18+BAO
	68% CL	95% CL	68% CL	95% CL
0.4	$0.91 \times 10^{-3} < \xi < 1.15 \times 10^{-3}$	$0.72 \times 10^{-3} < \xi < 1.19 \times 10^{-3}$	$0.87 \times 10^{-3} < \xi < 1.15 \times 10^{-3}$	$0.67 \times 10^{-3} < \xi < 1.19 \times 10^{-3}$
0.7	$2.22 \times 10^{-3} < \xi < 2.63 \times 10^{-3}$	$1.89 \times 10^{-3} < \xi < 2.71 \times 10^{-3}$	not consistent	$2.08 \times 10^{-3} < \xi < 2.66 \times 10^{-3}$
1	not consistent	$5.15 \times 10^{-3} < \xi < 6.30 \times 10^{-3}$	not consistent	not consistent

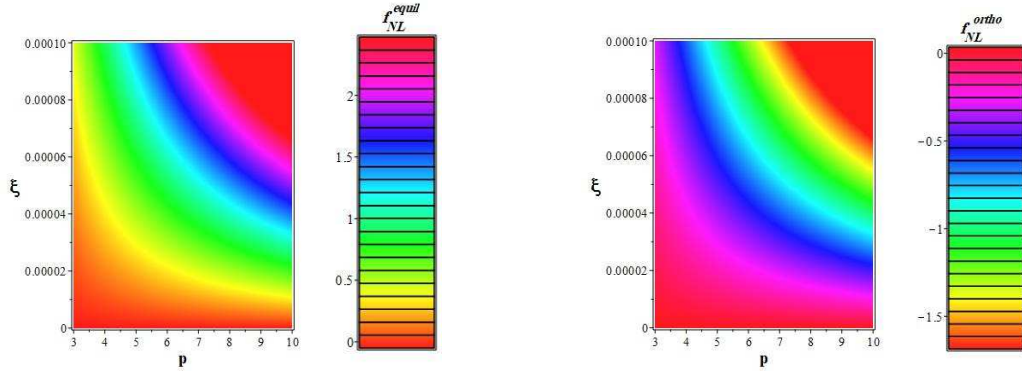


Figure 6: The prediction of the SFI model for equilateral and orthogonal amplitudes of the non-Gaussianity.

Table 2: The ranges of the parameter  $\xi$  in which the tensor-to-scalar ratio and the scalar spectral index of the non-minimal SFI are consistent with different data sets.

$p$	Planck2018 TT,TE,EE+lowE +lensing+BK14+BAO	Planck2018 TT,TE,EE+lowE +lensing+BK14+BAO	Planck2018 TT,TE,EE+lowE lensing+BK18+BAO	Planck2018 TT,TE,EE+lowE lensing+BK18+BAO
	68% CL	95% CL	68% CL	95% CL
0.92	$0 < \xi < 0.50 \times 10^{-5}$	$0 < \xi < 1.85 \times 10^{-4}$	$0 < \xi < 0.50 \times 10^{-5}$	$0 < \xi < 1.25 \times 10^{-4}$
0.95	$0 < \xi < 2.10 \times 10^{-5}$	$0 < \xi < 1.92 \times 10^{-4}$	$0 < \xi < 2.10 \times 10^{-5}$	$0 < \xi < 1.34 \times 10^{-4}$
0.98	$0 < \xi < 3.30 \times 10^{-5}$	$0 < \xi < 1.98 \times 10^{-4}$	$0 < \xi < 3.30 \times 10^{-5}$	$0 < \xi < 1.44 \times 10^{-4}$

## 5 Conclusion

In this paper, we have studied the inflation and primordial perturbations in a non-minimal model in order to compare LFI and SFI models in this background. We have presented the main background equations and also slow-roll parameters in the non-minimal inflation model. By considering the linear perturbations, we have obtained the scalar spectral index and tensor-to-scalar ratio in our setup. We have shown that both these parameters are modified in the presence of the non-minimal coupling between the scalar field and Ricci scalar. By extending the perturbations to the higher order and using the three-point correlation function, we have obtained the nonlinearity parameters in the non-minimal model. Then, we have expressed the amplitude of the non-Gaussianity in the equilateral and orthogonal configurations. After that, we have adopted two types of potentials, corresponding to the large field inflation and small field inflation. With these adoptions and with the non-minimal coupling function as  $\xi\phi^2$ , we have performed a numerical analysis on this non-minimal inflation model in order to see the status of LFI and SFI in this non-minimal setup. We have found that although the minimal large field inflation with  $N = 60$  is not consistent with new observational data, the presence of the non-minimal coupling makes it observationally viable. We have shown also that the non-minimal LFI model is consistent with both Planck2018 TT, TE, EE+lowE+lensing+BAO+BK14 and Planck2018 TT, TE, EE+lowE+lensing+BAO+BK18 data, if  $\xi \sim 10^{-3}$ . By analyzing the non-minimal SFI model, we have found that this model is observationally viable if  $\xi \lesssim 10^{-4}$ . Also, despite considering the non-minimal coupling, the tensor-to-scalar ratio in SFI is yet small. For both non-minimal LFI and SFI, we have studied equilateral and orthogonal non-Gaussianity and obtained small values for these parameters. Of course, these small values are consistent with Planck2018 TTT, EEE, TTE and EET data. The interesting result is that the absolute values of  $f_{NL}$ 's in both studied configurations are larger in the LFI than the SFI case. We note also that while to satisfy the condition  $\Delta\phi > M_{pl}$ , the value of  $p$  in LFI potential should be in the range  $[0.2, 5]$ , but our non-minimal setup constraints this condition even more severely as  $p \leq 0.92$  at 68% CL and  $p \leq 1.05$  at 95% CL with Planck2018 TT, TE, EE+lowE+lensing+BAO+BK14 data and  $p \leq 0.69$  at 68% CL and  $p \leq 0.080$  at 95% CL with Planck2018 TT, TE, EE+lowE+lensing+BAO+BK18 data. Similarly, for SFI potential, while usually  $p$  is constrained as  $p \in [2, 10]$ , in our non-minimal SFI model it is even more severely constrained as  $p \geq 9.1$  at 68% CL and  $p \geq 6.2$  at 95% CL with Planck2018 TT, TE, EE+lowE+lensing+BAO+BK14 data and  $p \geq 7$  at 68% CL and  $p \geq 6.2$  at 95% CL with Planck2018 TT, TE, EE+lowE+lensing+BAO+BK18 data. Finally, we note that this kind of study may be extended to the cases that the scalar field arises from holographic considerations and correspondences with, for instance, holographic dark energy models [39, 40].

## Authors' contributions

All authors have the same contribution.

## Data Availability

All data generated or analyzed during this study are included in this article.

## Conflicts of Interest

The authors declare that there is no conflict of interest.

## Ethical Considerations

The authors have diligently addressed ethical concerns, such as informed consent, plagiarism, data fabrication, misconduct, falsification, double publication, redundancy, submission, and other related matters.

## Funding

This research did not receive any grant from funding agencies in the public, commercial, or non-profit sectors.

## References

- [1] A. H. Guth, "Inflationary universe: A possible solution to the horizon and flatness problems", *Phys. Rev. D* **23**, 347 (1981). DOI: 10.1103/PhysRevD.23.347
- [2] A. D. Linde, "A new inflationary universe scenario: A possible solution of the horizon, flatness, homogeneity, isotropy and primordial monopole problems", *Phys. Lett. B* **108** (1982). DOI: 10.1016/0370-2693(82)91219-9
- [3] A. Albrecht and P. Steinhardt, "Cosmology for Grand Unified Theories with Radiatively Induced Symmetry Breaking", *Phys. Rev. Lett.* **48**, 1220 (1982). DOI: 10.1103/PhysRevLett.48.1220
- [4] A. D. Linde, *Particle Physics and Inflationary Cosmology*. Harwood, Chur, Switzerland (1990).
- [5] A. Liddle and D. Lyth, *Cosmological Inflation and Large-Scale Structure*. Cambridge University Press (2000).

- [6] J. E. Lidsey et al, “Reconstructing the inflaton potential—an overview”, *Rev. Mod. Phys.* **69**, 373 (1997). DOI: 10.1103/RevModPhys.69.373
- [7] A. Riotto, “Inflation and the theory of cosmological perturbations”, *ICTP Lect. Notes Ser. 14* (2003) 317-413, [arXiv: hep-ph/0210162]. DOI: 10.48550/arXiv.hep-ph/0210162
- [8] D. H. Lyth and A. R. Liddle, *The Primordial Density Perturbation*. Cambridge University Press (2009).
- [9] J. M. Maldacena, “Non-gaussian features of primordial fluctuations in single field inflationary models”, *JHEP* **0305**, 013 (2003). DOI: 10.1088/1126-6708/2003/05/013
- [10] N. D. Birrell and P. C.W. Davies, *Quantum Fields in Curved Space*. Cambridge Univ Press (1982).
- [11] V. Faraoni, “Nonminimal coupling of the scalar field and inflation”, *Phys. Rev. D* **53**, 6813 (1996). DOI: 10.1103/PhysRevD.53.6813
- [12] V. Faraoni, “Inflation and quintessence with nonminimal coupling”, *Phys. Rev. D* **62**, 023504 (2000). DOI: 10.1103/PhysRevD.62.023504
- [13] A. Zee, “Broken-Symmetric Theory of Gravity”, *Phys. Rev. Lett.* **42**, 417 (1979). DOI: 10.1103/PhysRevLett.42.417
- [14] F. S. Accetta, D. J. Zoller and M. S. Turner, “Induced-gravity inflation”, *Phys. Rev. D* **31**, 3046 (1985). DOI: 10.1103/PhysRevD.31.3046
- [15] S. Randjbar-Daemi, A. Salam, and J. Strathdee, “On Kaluza-Klein cosmology”, *Phys. Lett. B* **135**, 388 (1984). DOI: 10.1016/0370-2693(84)90300-9
- [16] T. Futamase and K. I. Maeda, “Chaotic inflationary scenario of the Universe with a nonminimally coupled ”inflaton” field”, *Phys. Rev. D* **39**, 399 (1989). DOI: 10.1103/PhysRevD.39.399
- [17] D. S. Salopek, J. R. Bond and J. M. Bardeen, “Designing density fluctuation spectra in inflation”, *Phys. Rev. D* **40**, 1753 (1989). DOI: 10.1103/PhysRevD.40.1753
- [18] R. Fakir and W. G. Unruh, “Improvement on cosmological chaotic inflation through nonminimal coupling”, *Phys. Rev. D* **41**, 1783 (1990). DOI: 10.1103/PhysRevD.41.1783
- [19] N. Makino and M. Sasaki, “The Density Perturbation in the Chaotic Inflation with Non-Minimal Coupling”, *Progress of Theoretical Physics*, **86**, 103 (1991). DOI: 10.1143/ptp/86.1.103
- [20] J. Hwang and H. Noh, “COBE constraints on inflation models with a massive non-minimal scalar field”, *Phys. Rev. D* **60**, 123001 (1999). DOI: 10.1103/PhysRevD.60.123001
- [21] S. Tsujikawa and H. Yajima, “New constraints on multifield inflation with nonminimal couplin”, *Phys. Rev. D* **62**, 123512 (2000). DOI: 10.1103/PhysRevD.62.123512
- [22] C. Pallis, N. Toumbas, “Non-minimal sneutrino inflation, Peccei-Quinn phase transition and non-thermal leptogenesis”, *JCAP* **1102**, 019 (2011). DOI: 10.1088/1475-7516/2011/02/019

- [23] K. Nozari and S. Shafizadeh, “Non-minimal inflation revisited”, *Physica Scripta*, **82**, 015901 (2010). DOI: 10.1088/0031-8949/82/01/015901
- [24] N. Aghanim, Y. Akrami, M. Ashdown, J. Aumont, C. Baccigalupi, “Erratum: Planck 2018 results: VI. Cosmological parameters”, *Astronomy and Astrophysics* **641**, A6 (2020). DOI: 10.1051/0004-6361/201833910e
- [25] Y. Akrami, F. Arroja, M. Ashdown, J. Aumont, C. Baccigalupi, “Planck 2018 results-X. Constraints on inflation”, *Astronomy and Astrophysics* **641**, A10 (2020). DOI: 10.1051/0004-6361/201833887
- [26] P. A. R. Ade, Z. Ahmed, M. Amiri, D. Barkats, R. B. Thakur, “Improved Constraints on Primordial Gravitational Waves using Planck, WMAP, and BICEP/Keck Observations through the 2018 Observing Season”, *Phys. Rev. Lett.* **127**, 151301 (2021). DOI: 10.1103/PhysRevLett.127.151301
- [27] D. Paoletti, F. Finelli, J. Valiviita and M. Hazumi, “Planck and BICEP/Keck Array 2018 constraints on primordial gravitational waves and perspectives for future B-mode polarization measurements”, *Phys. Rev. D* **106**, 083528 (2022). DOI: 10.1103/PhysRevD.106.083528
- [28] Y. Akrami, F. Arroja, M. Ashdown, J. Aumont, C. Baccigalupi, “Planck 2018 results. IX. Constraints on primordial non-Gaussianity”, *Astronomy and Astrophysics*, **641**, A9 (2019). DOI: 10.1051/0004-6361/201935891
- [29] J. Bardeen, “Gauge-invariant cosmological perturbations”, *Phys. Rev. D* **22**, 1882 (1980). DOI: 10.1103/PhysRevD.22.1882
- [30] V. F. Mukhanov, H. A. Feldman, R. H. Brandenberger, “Theory of cosmological perturbations”, *Physics Reports* **215**, 203 (1992). DOI: 10.1016/0370-1573(92)90044-Z
- [31] Daniel Baumann, “TASI Lectures on Inflation”, [arXiv:0907.5424] (2009). DOI: 10.48550/arXiv.0907.5424
- [32] A. De Felice and S. Tsujikawa, “Inflationary non-Gaussianities in the most general second-order scalar-tensor theories”, *Phys. Rev. D* **84**, 083504 (2011). DOI: 10.1103/PhysRevD.84.083504
- [33] A. De Felice and S. Tsujikawa, “Primordial non-gaussianities in general modified gravitational models of inflation”, *JCAP* **1104**, 029 (2011). DOI: 10.1088/1475-7516/2011/04/029
- [34] C. Cheung, P. Creminelli, A. L. Fitzpatrick, J. Kaplan and L. Senatore, “The effective field theory of inflation”, *JHEP* **0803**, 014 (2008). DOI: 10.1088/1126-6708/2008/03/014
- [35] D. Seery and J. E. Lidsey, “Primordial non-Gaussianities in single-field inflation”, *JCAP*, **0506**, 003 (2005). DOI: 10.1088/1475-7516/2005/06/003
- [36] A. De Felice, S. Tsujikawa, “Shapes of primordial non-Gaussianities in the Horndeski’s most general scalar-tensor theories”, *JCAP*, **03**, 030 (2013). DOI: 10.1088/1475-7516/2013/03/030
- [37] J. Martin, C. Ringeval, R. Trotta & V. Vennin, “The best inflationary models after Planck”, *JCAP*, **1403**, 039 (2014). DOI: 10.1088/1475-7516/2014/03/039

- [38] L. Senatore, "Lectures on inflation", Theoretical Advanced Study Institute in Elementary Particle Physics: new frontiers in fields and strings (2016).
- [39] S. Maity, P. Rudra, "Inflation driven by Barrow holographic dark energy", *JHAP* **2** (1), 1-12 (2022), DOI: 10.22128/jhap.2022.464.1012
- [40] S. Upadhyay, "Bouncing universe for deformed non-minimally coupled inflation model", *JHAP* **3** (1), 57-70 (2023), DOI: 10.22128/jhap.2023.651.1038